Supplementary Information

Synergistic Cobalt-MOF@rGO Nanocomposites for High-Performance Supercapacitors and Electrochemical Detection of Cd^{2+} ions

Ajay Kumar,[1,a,b,c] Jaiveer Singh,[1,a] Arushi Sharma,[a] Subhas C. Sahoo,[a] S.K. Mehta,[a] Vinod Kumar,[d] Oussama-El-Kadri[b,c,e], Shweta Rana[*a] and Ramesh Kataria[*a]

[a]*Department of Chemistry and Centre for Advanced Studies in Chemistry, Panjab University, Chandigarh-160 014, India*

[b]*Department of Biology, Chemistry, and Environmental Sciences, American University of Sharjah, POB 26666, Sharjah, United Arab Emirates*

[c]*Materials Research Center, College of Arts and Sciences, American University of Sharjah, 26666, Sharjah, United Arab Emirates*

[e]*Materials Science and Engineering PhD Program, College of Arts and Sciences, American University of Sharjah, 26666, Sharjah, United Arab Emirates*

[d]*Department of Chemistry, Central University of Haryana, Mahendragarh-123031*

[1]*Co-first authors*

***Email:** rkataria@pu.ac.in; shweta0402@gmail.com*

Content:

S.No.	Figures
Section S1	Experimental section
Figure S1	FTIR spectra of NADP
Figure S2	FTIR spectra of ligand (L_1)
Figure S2 (a)	Spherical void created by the paddlewheel SBUs in wireframe and
Figure S2 (b)	(b) space-filled form.
Figure S4	FESEM mapping and EDS results of PUC6@rGO.
Figure S5	(a) Current (i)/[scan rate (ν)]$^{1/2}$ vs [scan rate(ν)$^{1/2}$] plot and (b) scan rate (ν) vs charge contribution (%) for PUC6@rGO based supercapacitor device
Figure S6	Nyquist plots for PUC6@rGO based symmetric supercapacitor device.
Figure S7	Nyquist plots for PUC6@rGO based symmetric supercapacitor device before and after GCD cycles.
Figure S8	Galvanostatic charge-discharge (GCD) profiles
Figure S9	Bode plot for PUC6@rGO based symmetric supercapacitor device
Table S1	Crystallographic parameters of PUC6
Table S2 (a)	Bond angles for PUC6
Table S2 (b)	Bond distance for PUC6

S1. Experimental Section

S1.1 Reagents

NADP was purchased from TCI Chemicals. Cobalt nitrate hexahydrate ($Co(NO_3)_2.6H_2O$), methanol, dimethylacetamide, acetic acid, graphene oxide, concentrated sulfuric acid (H_2SO_4), sodium nitrate ($NaNO_3$), hydrogen peroxide (H_2O_2), sodium carbonate (Na_2CO_3), sodium borohydride ($NaBH_4$), and potassium hydroxide (KOH) were obtained from Sigma-Aldrich. All reagents were of analytical grade and used without further purification. Solutions were prepared using triple-distilled water throughout the experiments.

S1.2 Instrumentation

Powder X-ray diffraction (PXRD) analysis was performed using a PANalyticalX'Pert PRO diffractometer equipped with Cu Kα radiation to examine the crystalline structure of the samples. Raman spectra were recorded on a Horiba Jobin Yvon LABRAM HR spectrometer. X-ray photoelectron spectroscopy (XPS) measurements were carried out using a PHI 5000 VersaProbe III instrument to investigate surface chemical composition and elemental states. Surface morphology and elemental distribution of the composite were analyzed using a field-emission scanning electron microscope (FE-SEM, Hitachi SU8010) coupled with energydispersive X-ray (EDX) spectroscopy. Electrochemical measurements were conducted using a Metrohm AUTOLAB PGSTAT20 N electrochemical workstation controlled by NOVA 2.1.4 software. A conventional three-electrode configuration was employed, in which the synthesized composite served as the working electrode, Ag/AgCl acted as the reference electrode, and a platinum wire was used as the counter electrode.

S1.3 Single-Crystal X-ray Diffraction Data Collection and Structure Determination

High-quality single crystals suitable for X-ray diffraction were obtained by slow crystallization from a solvent system comprising DMF.A selected crystal of PUC-6 was mounted on a Hampton cryoloop and analyzed using a SuperNova single-crystal X-ray diffractometer equipped with a microfocused sealed Mo X-ray tube (Mo-Kα radiation, λ = 0.71073 Å) and a HyPix3000 area detector. Intensity data were collected through ω-scan measurements with an incremental step size of 0.3° per frame and an exposure time of 10 s per frame.

Data acquisition, integration, and reduction were performed using the CrysAlisPro software package, while structure visualisation and further processing were carried out with Olex2. The initial crystal structure solution was achieved by direct methods using the SIR2004 program, followed by full-matrix least-squares refinement employing the SHELXL refinement suite[2,3]. All non-hydrogen atoms were refined anisotropically.

The presence of highly disordered lattice solvent molecules (DMF and water) resulted in diffuse electron density that could not be reliably modelled. Consequently, the solvent contribution-corresponding to two DMF and three water molecules per unit cellwas treated using the solvent masking procedure implemented in Olex2. As a result, the reported molecular composition of the coordination framework may show minor deviations from the actual formulation.

The crystallographic data for this structure, excluding structure factors, have been deposited with the Cambridge Crystallographic Data Centre (CCDC) under deposition number 2467429**.** Complete crystallographic information files (CIFs) can be obtained free of charge from the CCDC, Cambridge, United Kingdom.

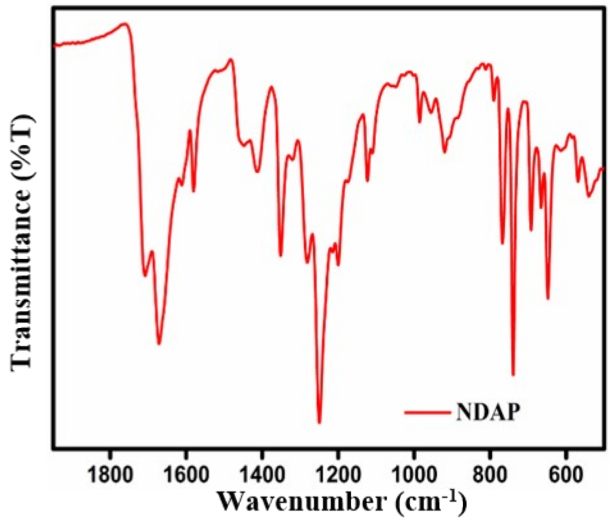

Figure S1.FTIR spectra of NADP

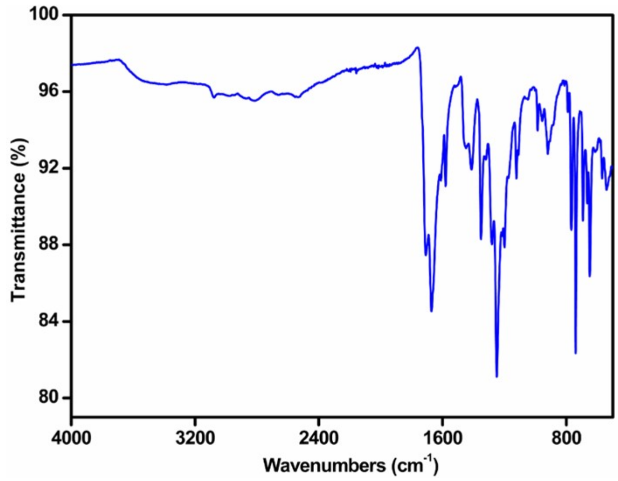

Figure S2.FTIR spectra of ligand (L_1)

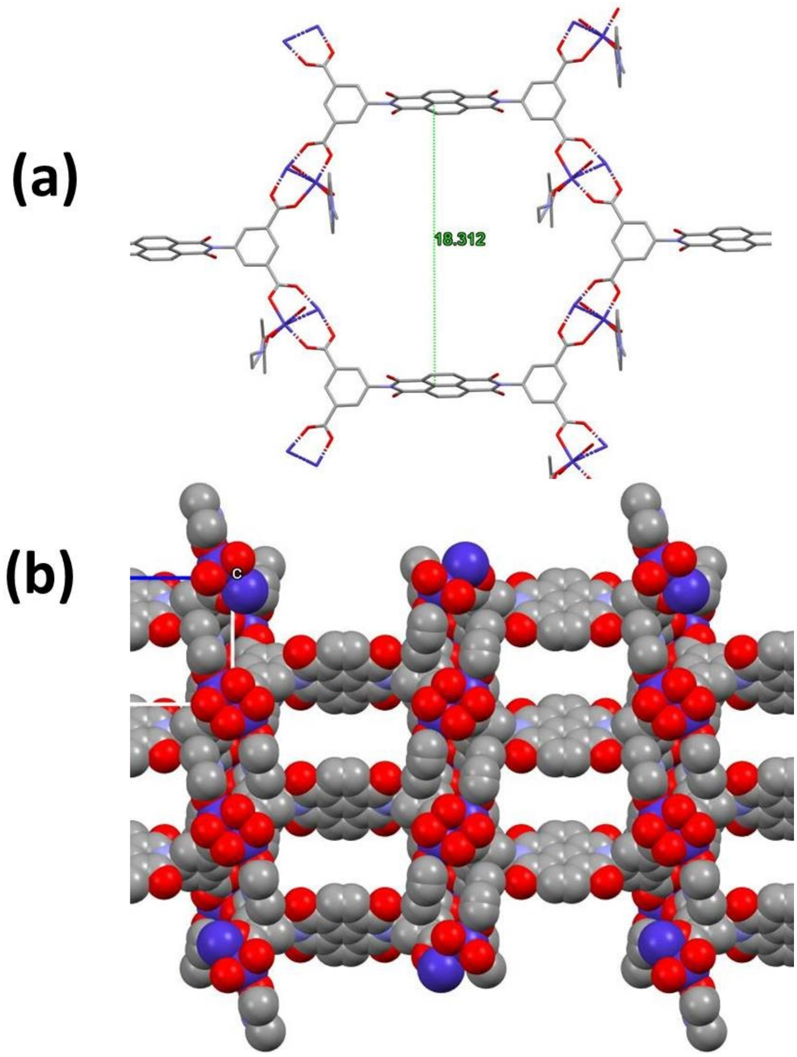

Figure S3. (a) Spherical void created by the paddlewheel SBUs in wireframe and (b) space-filled form

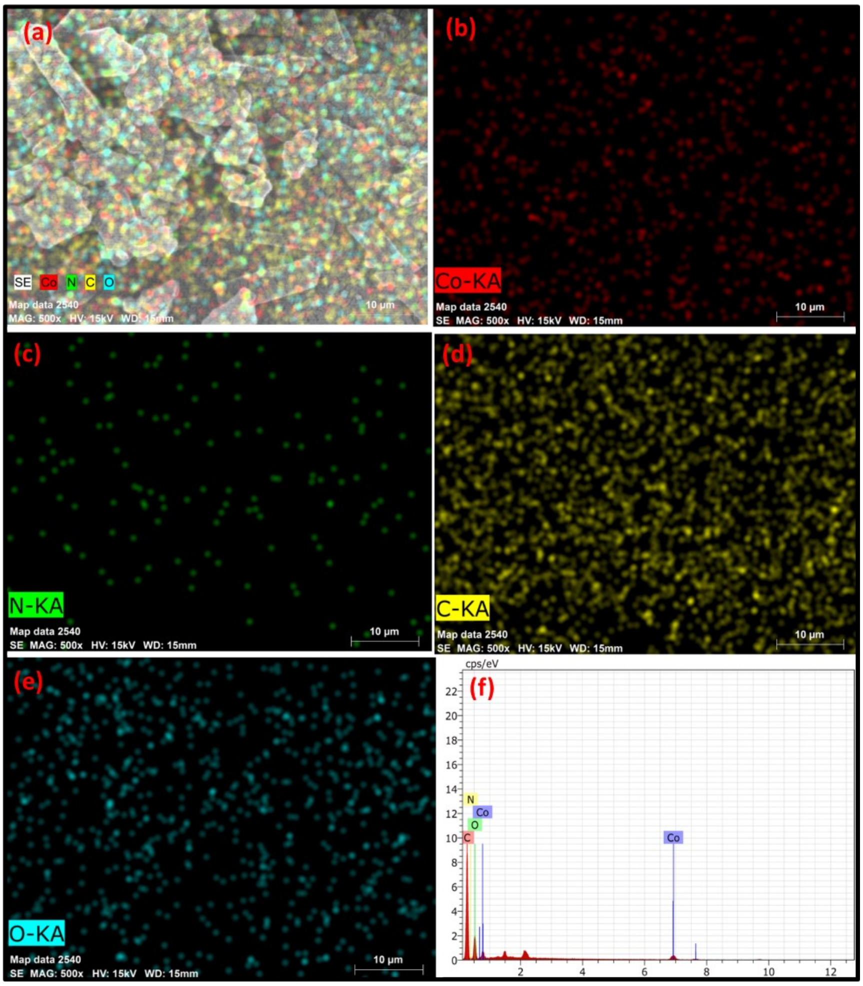

Figure S4. FESEM mapping and EDS results of PUC6@rGO

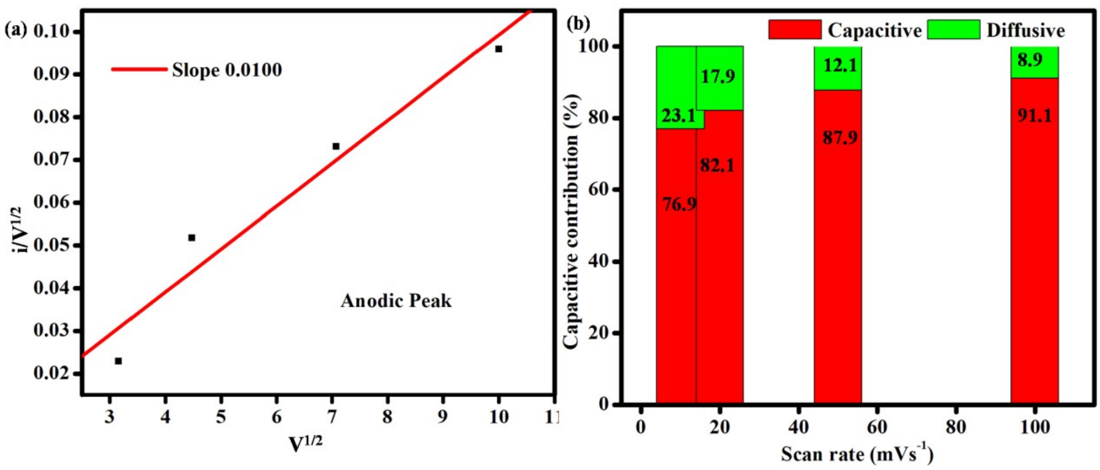

Figure S5. (a) Current (i)/[scan rate (ν)]$^{1/2}$ vs [scan rate(ν)$^{1/2}$] plot and (b) scan rate (ν) vs charge contribution (%) for PUC6@rGO based supercapacitor device.

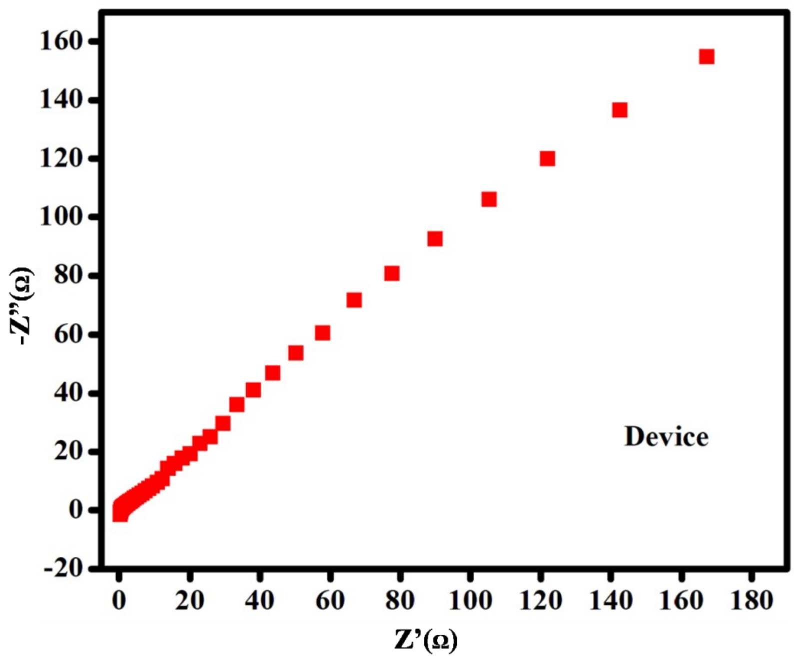

Figure S6 Nyquist plots for PUC6@rGO based symmetric supercapacitor device.

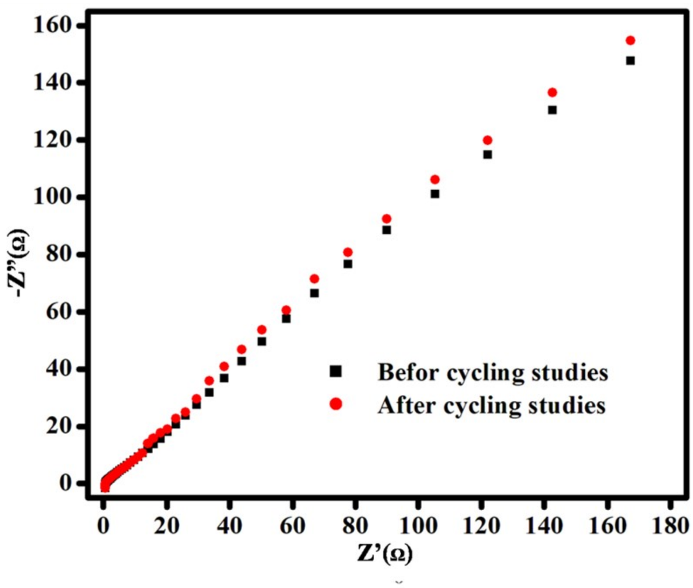

Figure S7 Nyquist plots for PUC6@rGO based symmetric supercapacitor device before and after GCD cycles.

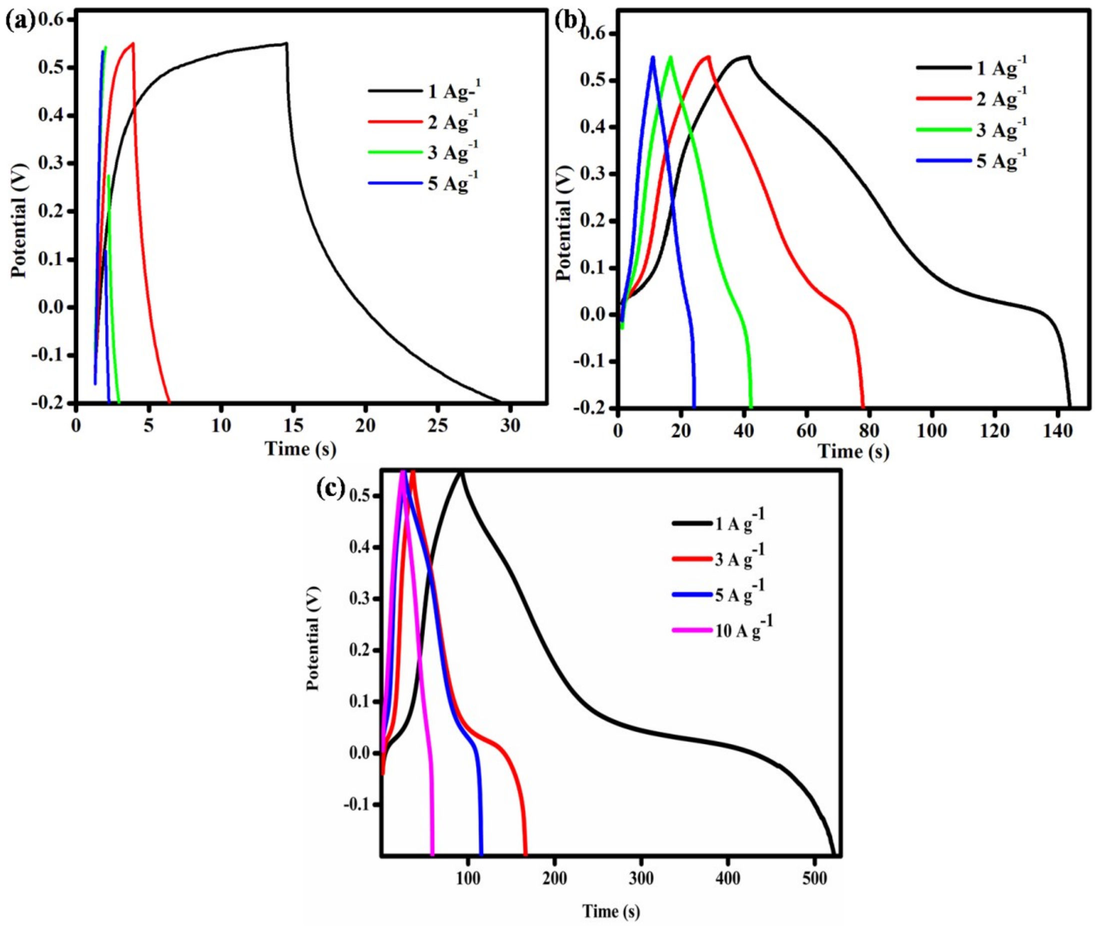

Figure S8. Galvanostatic charge-discharge (GCD) profiles for (a) PUC6, (b) rGO and (c) PUC6@rGO at a current density of 1 A g^{-1}; (d) GCD curves of PUC6@rGO at various current densities ranging from 1 to 5 A g^{-1}.

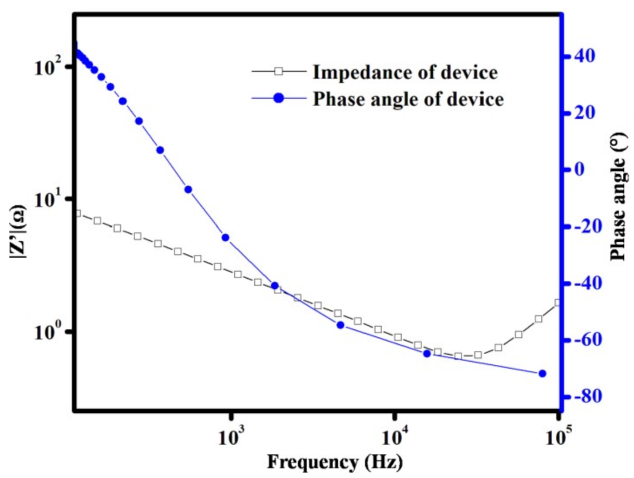

Figure S9. Bode plot for PUC6@rGO based symmetric supercapacitor device.

Table S1: Crystallographic parameters of PUC6

Identification code	**PUC6**
CCDC	2467429
Empiricalformula	$C_{18.75}H_{5.90}Co_4N_2O_7$
M_r [g mol^{-1}]	430.08
T (K)	293(2)
wavelength (A°)	0.71073
crystal system	Monoclinic
space group	*I2/m*
a [Å]	10.5576(6)
b [Å]	14.9621(9)
c [Å]	36.9093(13)
α [deg]	90
β [deg]	90.034(5)
γ [deg]	90
V [Å^3]	5830.3(5)
Z	8
ρ_{calc}[g cm^{-3}]	0.980
μ [mm^{-1}]	0.617
F (000)	1727
crystal size [mm]^3	0.12 × 0.008 × 0.005
reflection collected	13769
independent reflections	5317
GOF on F^2	1.096
final R indices(R1/wR2) [I > 2σ(I)]	0.1176/ 0.3074
R indices (R1/wR2) all data	0.2086/ 0.3704

Table S2 (a): Bond angles for PUC6

Atom	**Atom**	**Atom**	**Angle/°**	**Atom**	**Atom**	**Atom**	**Angle/°**
$O3^1$	Co1	$O3^2$	88.4(3)	C14	C12	C11	121.0(9)
$O4^3$	Co1	$O3^1$	160.9(3)	C14	C12	C13	120.0(10)
$O4^3$	Co1	$O3^2$	88.3(3)	$C11^7$	C11	C12	120.1(11)
O4	Co1	$O3^1$	88.3(3)	C10	C11	C12	120.4(8)
O4	Co1	$O3^2$	160.9(3)	C9	C10	C11	119.0(10)
$O4^3$	Co1	O4	88.6(4)	$C15^7$	C10	C11	121.0(8)
O7	Co1	$O3^2$	96.1(3)	$C15^7$	C10	C9	120.0(9)
O7	Co1	$O3^1$	96.1(3)	O6	C13	N1	121.4(9)
O7	Co1	O4	103.0(3)	C12	C13	N1	118.0(9)
O7	Co1	$O4^3$	103.0(3)	C12	C13	O6	120.6(11)
$O2^4$	Co2	$O2^5$	87.7(3)	O5	C9	N1	119.8(8)
O1	Co2	$O2^5$	89.2(2)	C10	C9	N1	119.6(10)
O1	Co2	$O2^4$	160.4(3)	C10	C9	O5	120.6(10)

O1^{6}	Co2	O2^{5}	160.4(3)	C15	C14	C12	119.2(11)
O16	Co2	O2^{4}	89.2(2)	C14	C15	C10^{7}	119.2(11)
O16	Co2	O1	87.1(4)	C16	N2	C17	156.0(10)
O8	Co2	O2^{5}	96.4(3)	C16^{3}	N2	C17	156.0(10)
O8	Co2	O2^{4}	96.4(3)	C16^{3}	N2	C16	48(2)
O8	Co2	O1	103.1(3)	C18^{3}	N2	C17	96.8(12)
O8	Co2	O1^{6}	103.1(3)	C18	N2	C17	96.8(12)
C8	O3	Co1	134.7(6)	C18	N2	C16^{3}	59.1(14)
C1	O2	Co2	134.3(7)	C18^{3}	N2	C16^{3}	107.1(18)
C1	O1	Co2	118.1(6)	C18^{3}	N2	C16	59.1(14)
C8	O4	Co1	117.3(6)	C18	N2	C16	107.1(18)
C19^{6}	O8	Co2	151.8(10)	C18	N2	C18^{3}	166(3)
C19	O8	Co2	151.8(10)	C19	N3	C19^{6}	45.0(18)
C19	O8	C19^{6}	43.4(17)	C21^{6}	N3	C19	136.6(16)
C16	O7	Co1	148.7(10)	C21	N3	C19^{6}	136.6(16)
C16^{3}	O7	Co1	148.7(10)	C21^{6}	N3	C19^{6}	164(3)
C16^{3}	O7	C16	46.5(18)	C21	N3	C19	164(3)
C2	C3	C4	121.9(6)	C21^{6}	N3	C21	36(2)
C13	N1	C6	117.0(7)	C18	C18A	C16^{3}	76(4)
C9	N1	C6	119.0(8)	N2	C16	O7	132.1(17)
C9	N1	C13	124.1(7)	C18A	C16	O7	110(2)
C5	C4	C3	117.7(7)	C18A	C16	N2	117(2)
C8	C4	C3	121.0(7)	C16^{3}	C16	O7	66.7(9)
C8	C4	C5	121.2(7)	C16^{3}	C16	N2	66.0(10)
C1	C2	C3	121.5(7)	C16^{3}	C16	C18A	175.3(19)
C7	C2	C3	118.7(7)	C18^{3}	C16	O7	145(2)
C7	C2	C1	119.7(7)	C18^{3}	C16	N2	82(2)
C6	C5	C4	119.5(7)	C18^{3}	C16	C18A^{3}	35.5(16)
C5	C6	N1	118.0(7)	N3^{6}	C19	O8^{6}	135.3(16)
C7	C6	N1	119.2(7)	C20A^{6}	C19	O8^{6}	122.9(19)
C7	C6	C5	122.8(7)	C20A^{6}	C19	N3^{6}	101.1(17)
O4	C8	O3	126.5(8)	C19^{6}	C19	O8^{6}	68.3(9)
C4	C8	O3	117.0(8)	C19^{6}	C19	N3^{6}	67.5(9)
C4	C8	O4	116.3(8)	C19^{6}	C19	C20A^{6}	168.6(14)
O1	C1	O2	126.9(8)	C18A	C18	N2^{3}	107(4)
C2	C1	O2	114.6(9)	C16^{3}	C18	N2^{3}	38.9(13)
C2	C1	O1	118.5(8)	C16^{3}	C18	C18A	68(3)
C6	C7	C2	119.0(7)	C21^{6}	C21	N3	72.2(12)
C13	C12	C11	118.9(9)				

Table S2 (b): Bond distance for PUC6

Atom	Atom	Length (Å)	Atom	Atom	Length (Å)
Co1	Co1^{1}	2.915(3)	C5	C6	1.368(11)
Co1	O3^{1}	2.045(5)	C6	C7	1.344(11)
Co1	O3^{2}	2.045(5)	O5	C9	1.263(12)
Co1	O4	2.008(6)	O6	C13	1.221(13)
Co1	O4^{3}	2.008(6)	C12	C11	1.387(14)
Co1	O7	1.983(10)	C12	C13	1.495(12)
Co2	Co2^{4}	2.909(3)	C12	C14	1.428(15)
Co2	O2^{5}	2.051(5)	C11	C11^{7}	1.396(15)
Co2	O2^{4}	2.051(5)	C11	C10	1.397(13)
Co2	O1	2.007(6)	C10	C9	1.472(11)
Co2	O1^{6}	2.007(6)	C10	C15^{7}	1.427(16)
Co2	O8	1.990(9)	C14	C15	1.389(13)
O3	C8	1.247(10)	N2	C17	1.42(3)
O2	C1	1.257(11)	N2	C16	1.15(2)
O1	C1	1.234(11)	N2	C16^{3}	1.15(2)
O4	C8	1.273(11)	N2	C18^{3}	1.81(4)
O8	C19^{6}	1.157(19)	N2	C18	1.81(4)
O8	C19	1.157(19)	N3	C19^{6}	1.12(2)
O7	C16	1.19(2)	N3	C19	1.12(2)
O7	C16^{3}	1.19(2)	N3	C21^{6}	1.56(4)
C3	C4	1.400(10)	N3	C21	1.56(4)
C3	C2	1.366(11)	C20A	C19^{6}	1.48(3)
N1	C6	1.470(8)	C18A	C16^{3}	1.50(4)
N1	C13	1.359(12)	C18A	C18	0.94(4)
N1	C9	1.326(13)	C16	C16^{3}	0.94(4)
C4	C5	1.392(9)	C16	C18^{3}	1.57(4)
C4	C8	1.475(11)	C19	C19^{6}	0.86(3)
C2	C1	1.497(11)	C21	C21^{6}	0.95(5)
C2	C7	1.411 (9)			

References:

1. M. C. Burla, R. Caliandro, M. Camalli, B. Carrozzini, G. L.Cascarano, C. Giacovazzo, M. Mallamo, A. Mazzone, G. Polidoriand R. Spagna, J. Appl. Crystallogr., 2012, 45, 357–361.
2. G. M. Sheldrick, Acta Crystallogr., Sect. C: Struct. Chem.,2015, 71, 3–8.
3. O. V. Dolomanov, L. J. Bourhis, R. J. Gildea, J. A. K. Howardand H. Puschmann, J. Appl. Crystallogr., 2009, 42, 339–341.